Research papers

Sensitivity of urban flood simulations to stormwater infrastructure and soil infiltration

Afrin Hossain Anni[a], Sagy Cohen[a,*], Sarah Praskievicz[b]

[a] *Department of Geography, University of Alabama, Tuscaloosa 35487, USA*
[b] *Department of Geography, Environment, and Sustainability, University of North Carolina at Greensboro, Greensboro 27402, USA*

ARTICLE INFO

ABSTRACT

Flooding from intense rainfall is a major hazard in many urban areas. One of the major challenges in urban flood simulations is lack of data about the location and properties of stormwater infrastructure and land cover. In this paper, we investigate the sensitivity of urban flood simulations to inputs of stormwater infrastructure and soil characteristics. We use a 2D hydrodynamic model (MIKE URBAN) to simulate flood events on the University of Alabama (UA) campus in Tuscaloosa U.S.A. Infiltration rate, soil moisture, and soil texture were measured in the field. Soil texture was found to be homogeneous across campus (sandy loam) but with a high degree of spatial and temporal variation in infiltration rate and soil moisture. Comparison between different storm event return periods (10, 25, 50, and 100 years) shows that the same flooding hotspots are persistent but with considerable variation in water depth and flood extent. To investigate the sensitivity of the simulations to stormwater infrastructure, simulations without the stormwater infrastructure input were conducted. The results show that stormwater infrastructure decreases flooding volume of RP 10, 25, 50, and 100 by factors of 20, 14, 12, and 8, respectively. This shows that urban flood simulation is highly sensitive to the inclusion of stormwater infrastructure, though with decreasing relative impact for larger events. To investigate the sensitivity of the simulations to soil characteristics, four land-cover simulations (actual, uniform, entirely pervious, entirely impervious) were compared. The results show flood simulation predictions are sensitive to both the value and spatial explicitness of the soil input data. We discuss challenges in urban flood simulation and their potential solutions in the context of emerging frameworks for national and global hyper-resolution flood forecasting and analysis.

1. Introduction

The effects of urban flooding on individuals and communities can be enormous especially when considering economic loss such as property loss; loss of hourly wages for those unable to reach their workplaces; hours lost in traffic rerouting and traffic challenges; disruptions in local, regional, and national supply chains; school closings with resultant impact on parents; sudden power outages; disruptions of communication systems; and contamination of water sources, spreading of water-related diseases and threats to human health (Weber, 2019; EPA, 2018; IPCC, 2014; Mahmood et al., 2017; Walsh et al., 2016; Brown and Murray, 2013; Hoang and Fenner, 2016; Curriero et al., 2001; Tunstall et al., 2006; Booth, 2012). In recent years, urban flooding due to extreme weather, rapid urbanization and climate change has been increasing both in severity and frequency worldwide, increasing risks to human lives, health, properties, infrastructure, and the environment

(Mahmood et al., 2017; Huong and Pathirana, 2013; Mahmoud and Gan, 2018; Di Baldassarre et al., 2010; Agbola et al., 2012; ActionAid, 2006; Ntelekos et al., 2010; Galloway et al., 2018; Teng et al., 2017).

Generally, urban flooding is caused by extreme runoff in a developed area where drainage is insufficient (Weber, 2019; Fernández and Lutz, 2010). This runoff travels over the surface, pooling in low-lying areas within the catchment until it drains, infiltrates, or evaporates. However, infiltration rates in the urban environment tend to be much lower than that of a natural environment due to prevalence of impervious land cover (Mahmoud and Gan, 2018; Villarini et al., 2011; Huong and Pathirana, 2013). Though urban stormwater infrastructure can drain surface water efficiently, it has a finite water transport capacity which can lead to waterlogging soon after a rainfall event commences (Fletcher et al., 2015; Schmitt et al., 2004; Hoang and Fenner, 2016). Several studies in recent years have focused on the role and significance of urban drainage systems and urban runoff, motivated

---

by the high costs and potential damage involved with prolonged flooding (Arnone et al., 2018; Grum et al., 2006; Arnbjerg-Nielsen, 2012; Berggren et al., 2014). According to the European Standard EN 752 (CEN, 1996, 1997), urban drainage systems should be designed to endure periods of flooding of 10–50 years, depending on the type of urban area and traffic infrastructure associated with it. However, aging drainage infrastructures and lack of upgrades to keep pace with development and climate changes can result in failure when extreme rainfall occurs. While improvement to stormwater infrastructure is costly, Stormwater Control Measures (SCMs) can be a cheaper solution to reduce the runoff from those locations (Li et al, 2017; Bell et al, 2016; Liu et al, 2014; National Research Council, 2009). There are different types of SCMs that are commonly used in urban environments to reduce runoff such as retention basin, bio-swales, infiltration trench, porous pavement, rain barrels, detention pond, green roof, rain garden (EPA, 2019). While these initiatives are quite promising for small rainfall events, the storm drainage network remains the dominant and most widely used technique in most urban environment.

This paper investigates urban flooding, using the University of Alabama (UA) campus in Tuscaloosa, Alabama, U.S.A. as a case study. UA experiences frequent flooding in several hotspots (Fig. 1). Like most urban environments, the UA campus has mixed land uses, i.e. a combination of green areas and human-made infrastructure. Runoff generated from the study area can vary spatially and temporally depending on the local drainage capacity, vegetation type and density, and topographic features.

Realistic calculation of runoff dynamics is dependent on accurate classification of the land cover, slope, topographic wetness index, and soil type, as well as other key soil properties (Nouh, 2006; Şen, 2004; Mahmoud and Gan, 2018). Runoff generation and accumulation depend on the effectiveness with which the surface is connected to the stormwater drainage system. For instance, in an urban environment, the impervious surfaces (buildings, roofs, roads, and parking lots) are often connected to an underground stormwater drainage system. For roads, parking lots, and similar types of surfaces, stormwater is collected through street curbs and gutters and eventually drains to the stormwater infrastructure network (DHI, 2015). However, there are some impervious surfaces that are less likely to be connected to the

stormwater infrastructure, such as sports fields, playgrounds, and paved paths, and when an extreme event occurs, they can get flooded within a short time span (Fig. 1).

GIS data on stormwater infrastructure is not readily available or attainable for most local urban environments, even in developed countries (Galloway et al, 2018; Liptan, 2017). Land-cover and soil characteristics can be inferred/estimated from soil or land-use/land-cover maps, or derived from remote sensing analysis, but these are often too coarse for urban applications. Given these limitations and the great efforts and costs involved in obtaining these data, such as through detailed surveys and digitization of infrastructure and land-cover maps and detailed field measurement and analysis of soil properties, elucidating the sensitivity of urban flood simulations to these factors is of great importance. While it is clear that stormwater infrastructure and soil properties are very important for accurate representation of urban water dynamics, their control on flooding dynamics during extreme events is not well understood. This is because soils may become saturated and stormwater infrastructure capacity may be reached shortly after the start of an event. This will limit or eliminate their effective influence on surface water dynamics. This paper aims to quantify the impact of stormwater infrastructure and soil properties on flood predictions by analyzing the sensitivity of urban flood simulations (using the MIKE URBAN model) to stormwater infrastructure and soil infiltration inputs under different storm severities (return periods of 10, 25, 50, and 100 years). We hypothesize that while the relative impact of these factors will decrease with increasing storm magnitude, they will remain highly impactful even for the most extreme storm severity.

2. Methodology

2.1. MIKE URBAN model

The combined hydrologic and hydraulic model MIKE URBAN (DHI, 2020) was used in this study to simulate surface water dynamics during rainstorm events on the UA campus. MOUSE is a powerful and wide-ranging engine used within MIKE for modelling complex hydrology and advanced hydraulics in both open and closed conduits, water quality and sediment transport for urban drainage systems, stormwater sewers,

Fig. 1. a and b: flood event on The University of Alabama (Tuscaloosa, AL) campus on 6th July 2018 near Bryant Denny Stadium and Tutwiler Hall (source: https://twitter.com/spann/status/1015375786604449792); c–e : flood event on campus on February 20, 2019 near the soccer stadium and behind the Bus Hub (picture by AHA).

and sanitary sewers (DHI user guide, 2017). Urban flood simulations using MIKE URBAN require the following model components:

MIKE URBAN – to model the 1D sewer network including the manholes and pipes;

MIKE ZERO – to generate a timeseries for rainfall data (in .dfs0 format) and to convert the digital elevation model (DEM) raster data to the model's native (DEM.dfs2) file format;

MIKE 21 – to model surface runoff/overland flow; and

MIKE FLOOD – to couple the 1D and 2D models.

The MOUSE engine provides tools to model surface runoff, infiltration, and evapotranspiration in urban catchments. The stepwise simulation procedure included the following steps: (a) rainfall-runoff simulation, (b) hydraulic network simulation and (c) 1D to 2D overland flow simulation. The outputs from the rainfall-runoff model are used as an input to the stormwater infrastructure network. Precipitation timeseries (prepared in MIKE ZERO) were applied over the urban catchments and transformed into surface runoff using the hydrological model. MOUSE Model B (kinematic wave model) was used, which includes Horton's infiltration equation for runoff simulation. It is the most popular runoff model for pervious area because it is conceptually simple and requires less detailed data (DHI user manual, 2015).

Hydrodynamic simulations in urban stormwater drainages can be performed under various boundary conditions (e.g., rainfall-runoff and external inflows to the network). In this study, only rainfall timeseries were used as the boundary condition to the MIKE model. Runoff, simulated in each sub-catchment, is drained into the stormwater network through catchment connections to the nearest inlets (nodes).

A 1D-2D coupling approach (MIKE FLOOD) was used in the simulations (Cadus and Poetsch, 2012). In the 1D drainage network model, runoff is simulated using the hydrologic model and inflows through the connected drainage channels. After that, the 2D model (MIKE 21) simulates overland flow throughout the catchment. This procedure allows for more accurate predictions of the flooded regions and the flood depth over the simulated domain. When underground stormwater drainage pipes are linked with overland surface runoff, the generated floodwater covers the surface after the drainage capacity of the stormwater system is reached.

2.2. Data

The data required and used in this study for modeling the 1D stormwater network and 2D surface hydraulics are:

a. Digital Elevation Model (DEM): 1-m LiDAR DEM (Fig. 2b). Obtained from the University of Alabama Planning Department.

b. Soil Infiltration: A field-measurement campaign was conducted to determine the soil properties of the study area and their seasonal variations (from September to December or fall to winter). Particle-size analysis and organic-matter content analyses were conducted to determine the characteristics of the soil that can affect its infiltration rates. Particle-size analysis was conducted using the USDA (2014) Soil Survey Manual. Two 25 g soil samples were analyzed from each location (Fig. 2d). For organic-matter analysis, soil samples were combusted at 500 °C for 5 h after being oven-dried at 100 °C for 12 h. Infiltration rates and soil-moisture conditions were measured under different antecedent-moisture conditions (dry and wet) to better represent the relevant parameters in the model and to analyze spatial and temporal trends in infiltration and its link to soil characteristics. Infiltration measurement using the Turf-Tech infiltrometer was conducted by inserting it at ~0.10 m deep into the soil. The duration and the amount of water used for each test was 15 min and ~1.5 L, respectively. Later, the data was converted to mm/hr. A total of 48 infiltration tests (12 for each location) were conducted. A Dynamax SM150 Portable Soil Moisture sensor was used for recording soil-moisture data. As the variability in soil moisture is high even in a small soil sample, an average of 10 soil-

moisture measurements was used for each location and time. In total, 480 (120 in each location) soil-moisture readings were collected over the study period.

c. Land use/land cover: ERDAS IMAGINE software was used for supervised classification (high-resolution (3-m) satellite imagery from Planetscope) to identify different land-cover types on campus such as buildings, roads, paths, parking lots, grass, and trees (Fig. 2c).

d. Precipitation: The 6th July 2018 storm event and design storms at RP of 10, 25, 50, and 100 years at 15-minute interval rainfall were compiled from the Tuscaloosa-Oliver Dam meteorological station (NOAA, 2018).

e. Stormwater Infrastructure: GIS data from UA was augmented with conduit geometry and length, pipe diameters, conveyances, manholes, nodes, junctions, and a network schematic (Fig. 2a). The network system consisted of 871 nodes (inlets) and 16 virtual outlets. The dimensions of the inlets are not available and so a constant value of 0.91 m (3 ft) is used for all inlets. The number of junctions in the network model was increased to 1731 to maintain a sloping direction of water in the pipe system. The number of pipe segments in the system is 2613, with varying length and diameter. The total length of pipes in the study area is 65,606 m.

2.3. Simulation scenarios and settings

A flooding event on 6th July 2018 was simulated and used to qualitatively evaluate the model results. This event was used as we were able to survey flooding locations during the event across the UA campus (e.g. Fig. 1c–e). Though the survey did not include all flooded locations, it offers confirmation of several flooding locations. This will allow us to evaluate whether or not these flooding locations were predicted by the model.

Design storms at return periods (RP) of 10, 25, 50, and 100 years were used to simulate flooding at different levels of severity. The stormwater infrastructure and measured soil characteristics are used in 'Realistic' simulations. The impact of the stormwater infrastructure on flood severity at varying RPs was quantified by comparing the Realistic simulations to simulations without the stormwater infrastructure input.

Infiltration input in the Realistic simulations was generated by dividing the study area into small sub-catchments where spatially varied infiltration rates collected from the field were averaged. The infiltration data for Tutwiler, Quad, Shelby Hall and Bryce Lawn ranged from 20 to 40 mm/hr, 60–120 mm/hr, 40–80 mm/hr and 35–60 mm/hr, respectively. The impact of soil characteristics on flood predictions was quantified by comparing the Realistic simulations to simulations with three soil infiltration input configurations:

1. Fully impervious – the entire study site was set to 0 mm/hr infiltration.

2. Fully pervious – the entire study site was set to high infiltration (maximum value of 120 mm/hr).

3. Uniform – the entire study site was set to a spatially uniform infiltration rate equal to the average infiltration rate of the Realistic simulation (53.6 mm/hr).

3. Results

3.1. Soil characteristics and distribution

The results of the particle-size analysis show that soil texture on campus can be classified as sandy loam. Soil texture was found to be relatively homogeneous across campus (Table 1), with a range of 24% (76%-52%) in the sand fraction and 24% (38%-14%) for clay. The infiltration rate for this soil type is high due to the relatively large proportion of sand particles, resulting in high porosity and permeability. According to Horton's initial infiltration capacity values for dry sand and loam with thick vegetation, the infiltration rate is expected to be 254 mm/hr and 152 mm/hr, respectively (DHI, 2015). These values
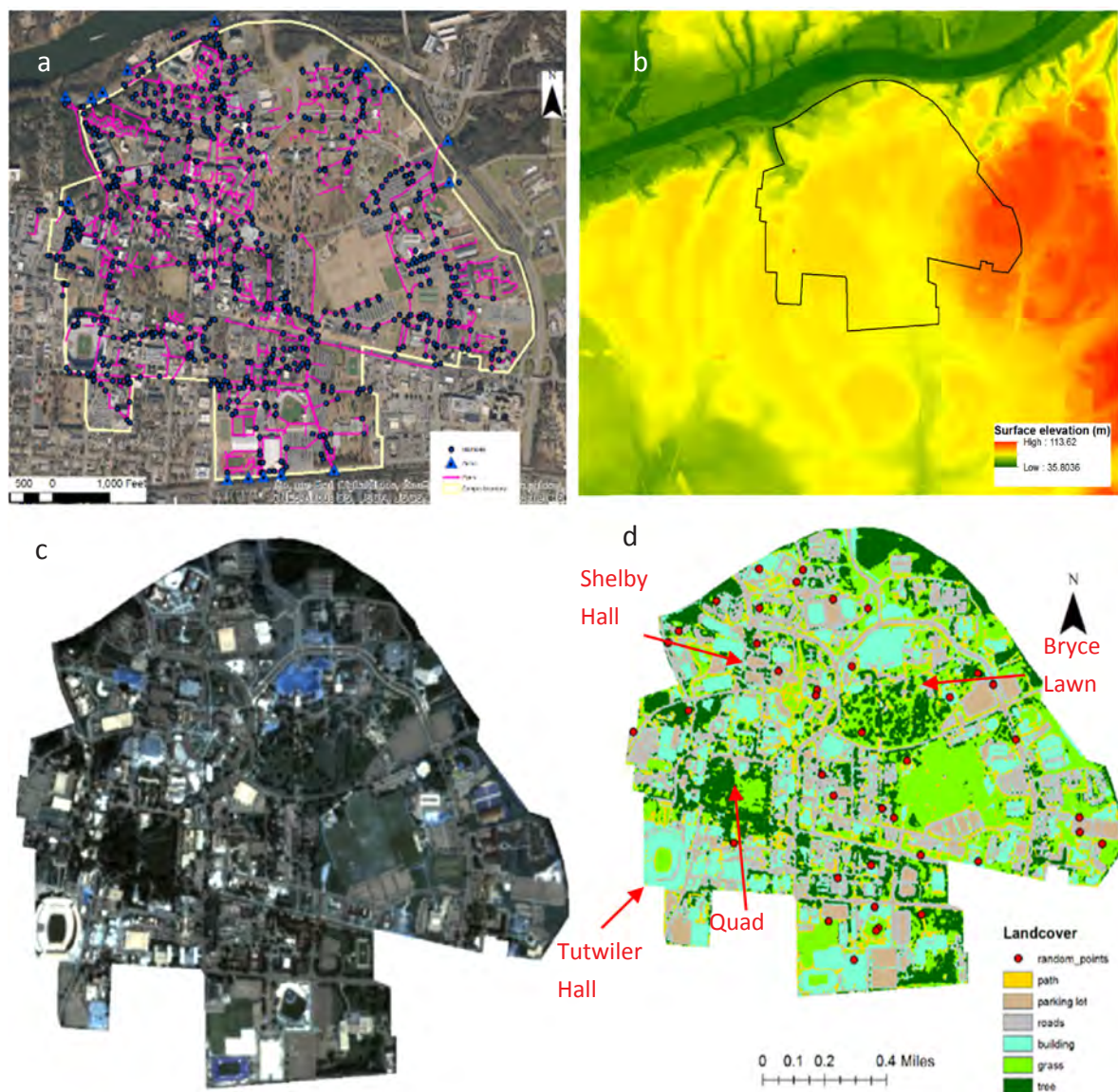
Fig. 2. (a) stormwater infrastructure system for UA; (b) DEM of the study site; (c) satellite imagery; (d) land cover classification.

Table 1
Particle size analysis and organic matter analysis results; two samples were collected in each location.

Sample	Sand (%)	Silt (%)	Clay (%)	Texture	OM (%) on 10/17/2018	OM (%) on 10/31/2018
Shelby 1	64	4	32	Sandy loam	2.6	3.8
Shelby 2	60	2	38	Sandy loam		
Quad 1	68	2	30	Sandy loam	2.6	3.6
Quad 2	60	2	38	Sandy loam		
Bryce Lawn 1	60	16	24	Sandy loam	2.7	3.8
Bryce Lawn 2	52	18	30	Sandy loam		
Tutwiler 1	76	10	14	Sandy loam	2.3	4.4
Tutwiler 2	68	10	22	Sandy loam		

Table 2
Soil moisture from gravimetric method and the SM 150 sensor.

Sample	% Water content − 16th October 2018		% Water content − 30th October 2018	
	Gravimetric	SM 150 sensor	Gravimetric	SM 150 sensor
Shelby Hall	14.4	16.0	17.9	19.2
Quad	9.0	8.9	11.0	11.0
Bryce Lawn	15.3	13.0	42.0	44.7
Tutwiler	12.5	12.9	19.9	20.8

correspond with the infiltration data collected from the field. Analysis of organic matter (% OM) was conducted, and it was also found to be homogeneous (Table 1). These values were within the typical range (1–5%) for upland soils (LJWORLD, 2019).

Gravimetric soil-moisture analyses were conducted in four locations on campus and repeated on days with different soil-moisture conditions. Soil-moisture readings from the SM150 sensor were compared to gravimetric soil-moisture measurements (Table 2). The soil moisture from the sensor was found to be within the range of ± 3% of the results from the gravimetric lab analysis. The soil moisture from the second day of measurements was higher due to rainfall earlier that week. The agreement between these two methods is high, so the SM150 sensor was further used for measuring soil moisture at the study sites. Among the four locations, the soil moisture at Bryce Lawn was found to be the
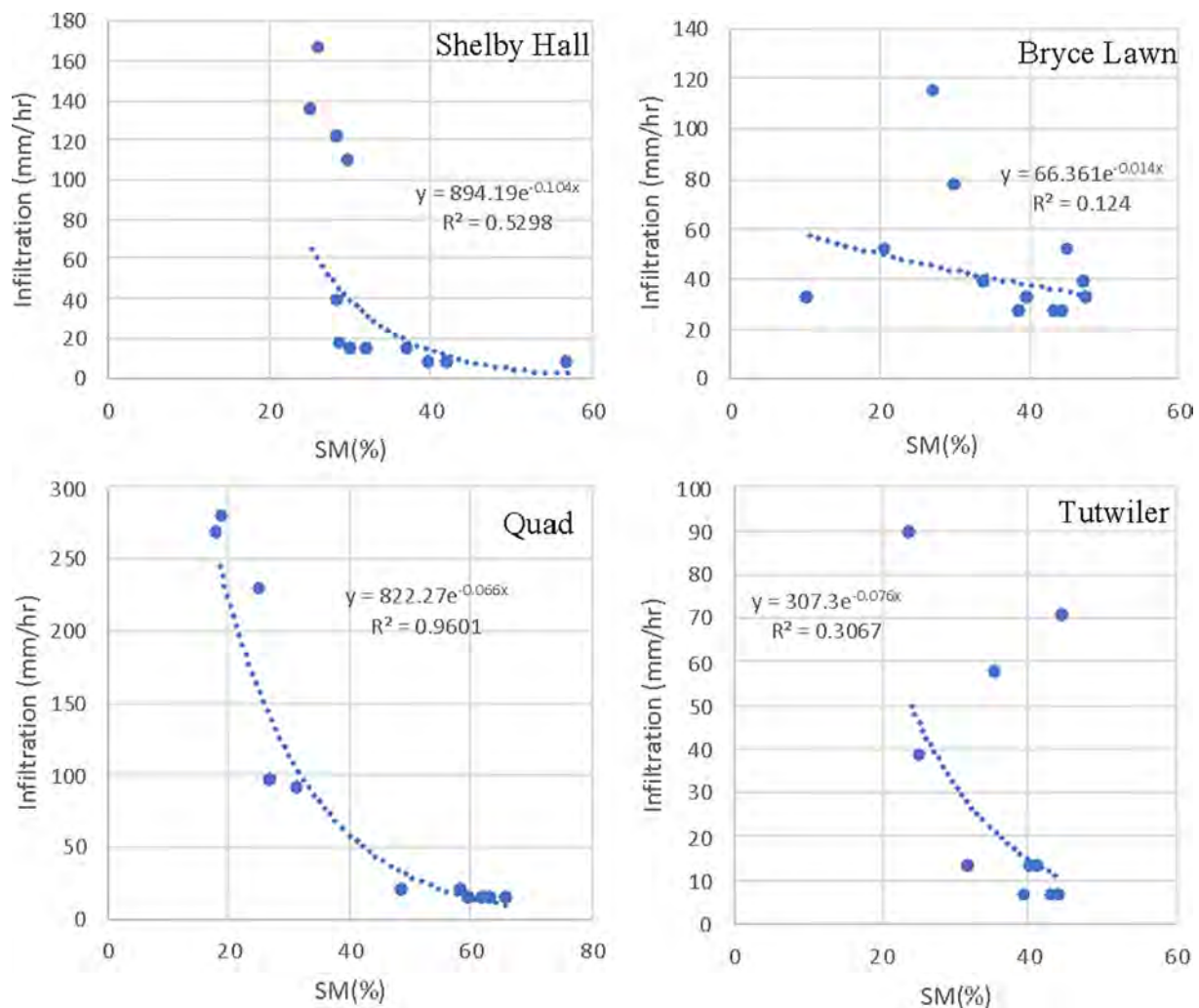
Fig. 3. Scatterplot of observed soil moisture and infiltration.

highest and the Quad was found to be the lowest in both tests (Table 2). This is interesting as both the Quad and Bryce Lawn are open green spaces. Differences in gravimetric soil moisture between the two dates also were the highest (15% − 9% = 6% and 42% − 11% = 31%, respectively) in these two locations. The proportion of fines (silt + clay) was higher at Bryce Lawn than the Quad (Table 1) and therefore the capacity to retain water was higher for Bryce Lawn. However, likely a more important reason for the difference between the two locations is the fact that soil on the Quad is more compacted because of intensive daily activities and foot traffic, including walking, recreational activities, and football game day activities. Wet soil increases the chance of soil compaction because soil moisture works as a lubricant between soil particles under pressure from traffic movement and daily activities (Al-Kaisi and Licht, 2005, Yang and Zhang, 2011).

An inverse relationship was found between soil moisture and infiltration. An increase in soil moisture results in a decrease in the infiltration rate and vice versa (Fig. 3). This relationship was strongest at Shelby and the Quad (R^2 = 0.53 and 0.96, respectively). These results show the non-stationarity and spatially variable co-dependence of soil moisture and infiltration rates, even for soils with similar texture and organic matter.

3.2. Model evaluation

A quantitative verification of model performance was not possible because of the lack of observed data on flood inundation. Measuring the

areal extent of flooded area during an actual event is difficult and dangerous. However, we did observe a flood event on campus on 6th July 2018 with a 4-hour rainfall event (between 4:00 pm to 8:00 pm), which yielded a total of 101 mm (equals a RP of about 7 years). We simulated this event to qualitatively compare the extent and spatial pattern of flooding with our observations of the actual event. We found that the simulated flooded area was 301,000 m^2 (the total area of the UA campus is 3,899,223 m^2). The ratio between flooded and non-flooded area was therefore 7.7%. The major inundated areas were near Tutwiler Hall with a flood depth of 0.78 m, behind the Biology building, and at the parking deck (also known as the Bus-Hub), where the flood depth was also 0.78 m (Fig. 4). These locations are adjacent to student/ fraternity housing. Toward the northeast side of the campus, the maximum inundation depth found near the parking lot just behind Cyber Hall and adjacent to Peter Bryce Boulevard was 0.35 m. Other than these locations, the flood water depth in different parts of campus was around 0.15 m. The model simulated locations and depths of flooding that corresponded very well with our observations of the actual event. This provides qualitative support for the model's ability to simulate flooding patterns on the UA campus.

3.3. Flooding under different precipitation return periods (RP)

Flooding caused by rainstorms at different return periods (RP; 10, 25, 50, and 100 years) was simulated (Fig. 5). Table 3 shows that, as expected, greater return periods yield greater floodwater volumes and
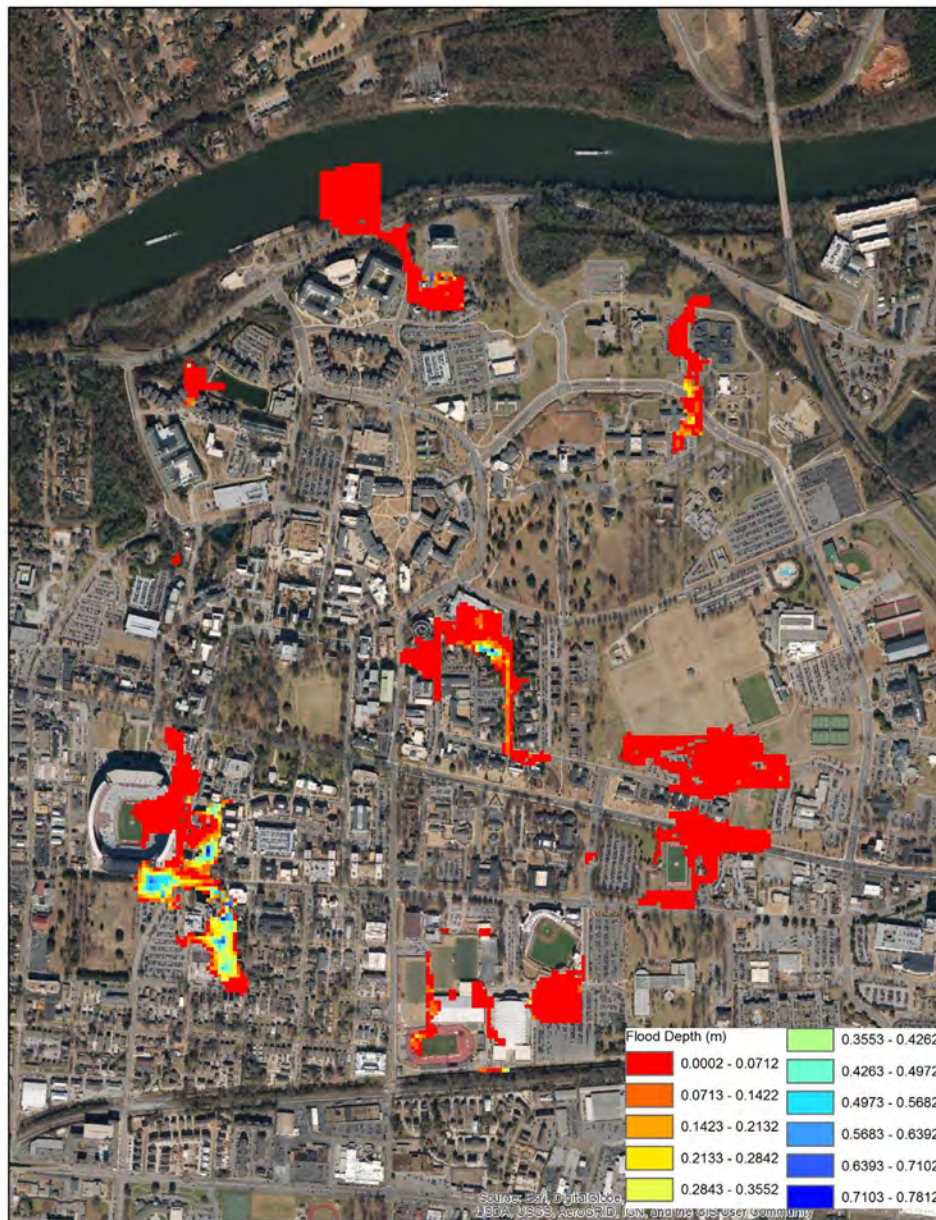
Fig. 4. Simulated flood inundation for 6th July 2018 event on University of Alabama campus.

depths. Flooding hotspots on campus were the same for all simulations, with increasing extent and water depth except for RP 10. For RP 10, two locations (the intersection near Bryant-Denny Stadium and Tutwiler and the Bus-Hub) were detected to be flooded with very negligible and dispersed waterlogging in some locations (Fig. 5). For RP 25 and 50, flood maps show similar patterns. The RP 100 flood map showed the highest flood volume and flooding at 10 different locations on campus with various depths and extents. The flood volume found for RP 100 was 4.8, 2.5, and 1.9 times higher than for RP 10, 25, and 50, respectively (Table 3).

3.4. The impact of stormwater infrastructure

A comparison between the simulations with and without stormwater infrastructure shows considerable differences in floodwater depth and extent throughout the study area (e.g., Fig. 6). The objective was to identify how important it is to include stormwater infrastructure to understand urban flood simulation performances under different storm severity scenarios. Due to the absence of detailed drainage data of

stormwater infrastructure, as is often the case in urban flood applications, instead of determining the exact carrying capacity, we quantified how it affects the flooding area and depth by comparing the differences between simulations with and without stormwater infrastructure. Floodwater volume without the stormwater infrastructure is higher by a factor of 20 for RP 10, and by factors of 14, 12, and 8 times for RP 25, 50, and 100, respectively (Table 4). The difference in volume between the two scenarios for RP 10 was found to be 348,864 m^3, which means that the simulated stormwater infrastructure was draining that volume of water in the 4-hour duration of the simulated storm event (~87,000 m^3/h). This translates to an average drainage capacity of 24 m^3/s.

These results demonstrate the importance of incorporating stormwater infrastructure into urban flood simulations. The reduction in the relative differences between the two simulation scenarios (with and without the stormwater infrastructure) with increasing storm RP can be explained by the finite drainage capacity of the stormwater infrastructure. The proportion of water drained by the stormwater infrastructure decreases for larger storms. However, these results show that
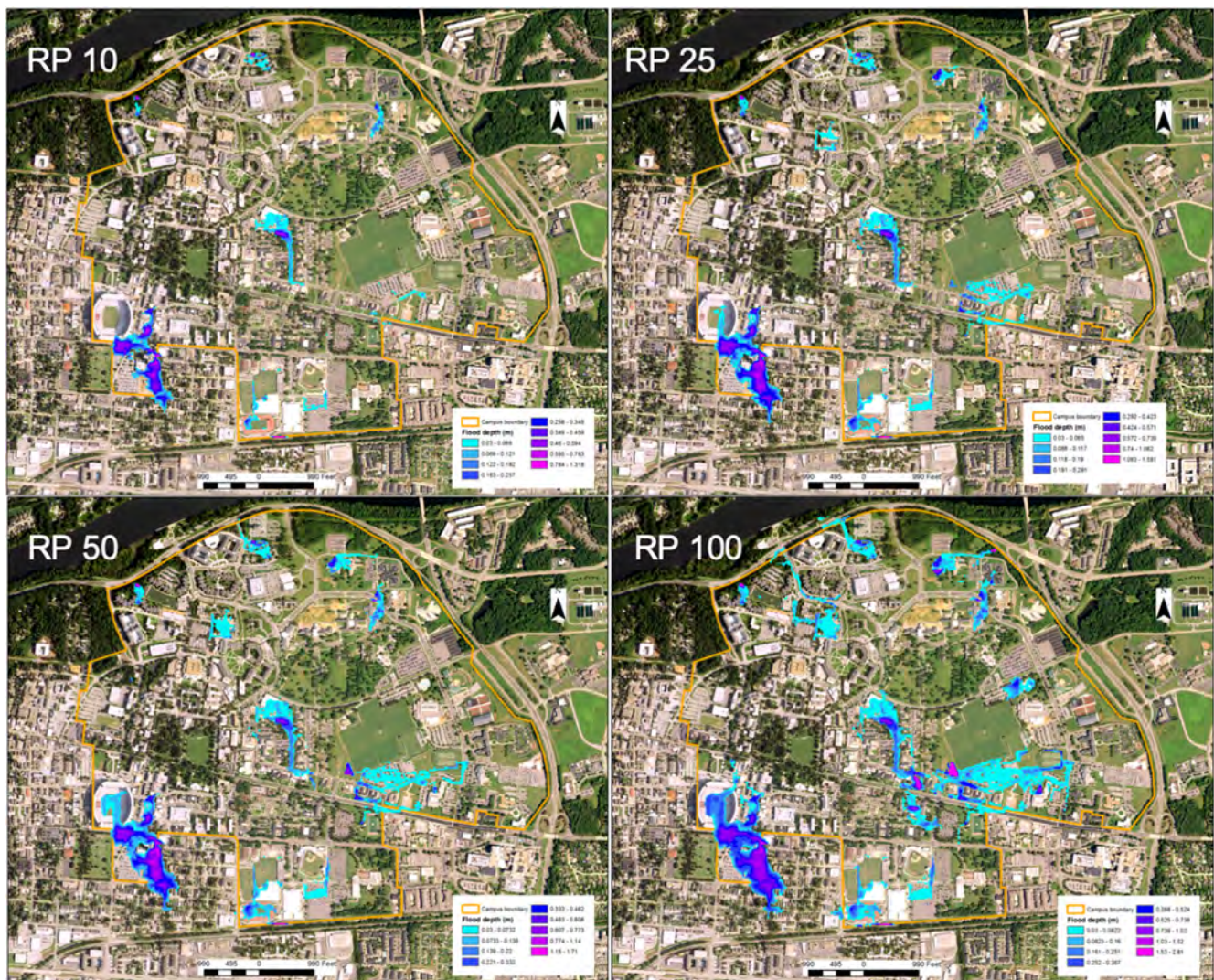
Fig. 5. Maximum floodwater depth maps for four RP scenarios.

even for RP 100, incorporating stormwater infrastructure into the simulation is crucial for predicting water volume and depth.

3.5. The impact of soil infiltration inputs

Three infiltration input configurations were compared to the Realistic scenario (spatially variable infiltration based on our field measurements and land-cover classification). The mean and maximum water depths found from the fully impervious flood simulations (for RP 25) were 0.21 m and 2.05 m, respectively (Fig. 7, Table 5). This is compared to the Realistic simulation with mean and maximum water depth of 0.19 and 1.58 m, a difference of 0.02 and 0.46 m, respectively. The simulated floodwater volume for the fully impervious simulation was 44,288 m^3, compared to 35,776 m^3 in the original simulation, a difference of 8512 m^3 (a difference factor of 1.2). For RP 100, the

floodwater volume for the fully impervious simulation was 97,280 m^3, compared to 88,960 m^3 in the original simulation, a difference of 8320 m^3 (a difference factor of 1.1). The fully pervious simulation (for RP 25) yielded mean and maximum flood depths of 0.13 m and 0.83 m, respectively (Table 5); a difference of 0.06 m and 0.75 m, respectively, from the Realistic simulation. The simulated floodwater volume for the pervious simulation (for RP 25) was 6208 m^3, a difference of 29,568 m^3 from the Realistic simulation (a difference factor of 0.17). For the RP 100 simulation, the floodwater volume for the fully pervious simulation was 30,280 m^3, a difference of 58,680 m^3 (a difference factor of 0.34).

The results of the uniform (average) infiltration scenario show a major reduction in floodwater volume relative to the Realistic simulation when simulating spatially uniform infiltration, a difference factor of 0.18 and 0.35 for RP 25 and 100, respectively (Table 5). This is surprising considering that the average infiltration across the study site

Table 3
Average floodwater statistics for RP 10, 25, 50, 100 and the 6th July 2018 event.

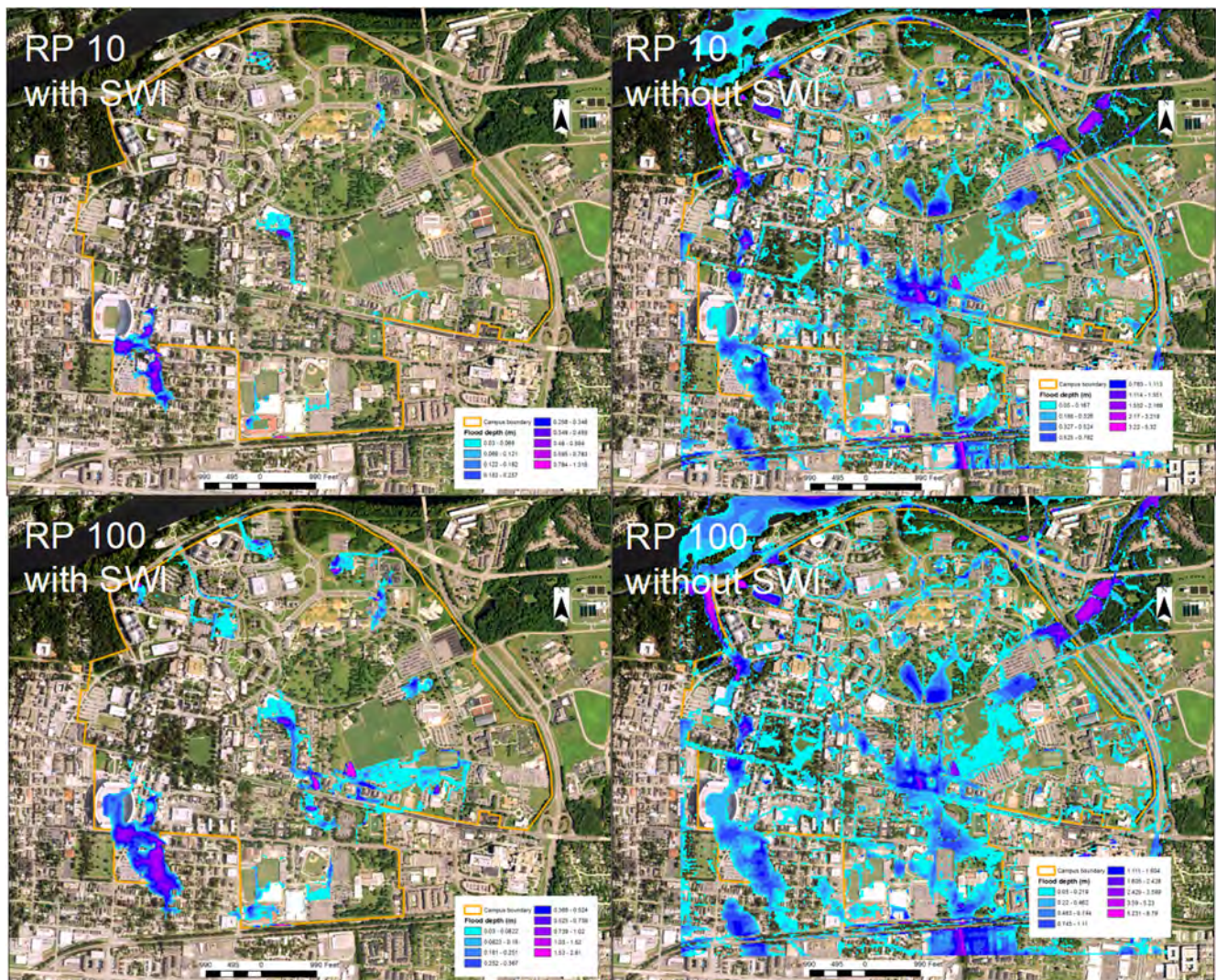| Flood scenario	No. of flooded cells	Average flood depth (m)	Maximum flood depth (m)	Total flood depth (m)	Volume (m^3)
RP 10	1575	0.18	1.32	289	18,496
RP 25	2990	0.19	1.58	559	35,776
RP 50	3812	0.19	1.71	710	45,440
RP 100	6194	0.23	2.81	1390	88,960
6th July 2018	3010	0.39	0.78	161	16,100

Fig. 6. Maximum floodwater depth maps for the simulations with and without stormwater infrastructure (SWI) for RP 10 and RP 100 scenarios.

is the same for the Realistic and uniform simulations. This can be attributed to the fact that flooding is most prevalent in areas dominated by impervious land cover, so using an average infiltration rate resulted in considerable underprediction in these hotspots. This effect is reduced in high-magnitude events (RP 100) due to a reduction in the relative contribution of infiltration to simulated surface water balance. These results, however, demonstrate that infiltration still has an impact, even for RP 100, yielding about one-third of the simulated floodwater volume (total volume of 31,232 m^3 and 88,960 m^3 for the uniform and Realistic simulations, respectively).

4. Discussion

The analysis of soil characteristics revealed highly homogeneous texture (sandy loam) and organic matter in the study site, but with a

high degree of spatial and temporal variation in soil moisture and infiltration rate. The soil moisture from the field observations was found to be lower with corresponding higher infiltration rates before November, but the soil moisture increased after November due to the increase in antecedent rain during November-December, which resulted in lower infiltration rates in the study area. These complex spatio-temporal dynamics in soil, even in areas with similar land-cover type, showcase the need for detailed soil data and for models that explicitly simulate soil moisture and infiltration dynamics. The value and spatial explicitness of the model's soil infiltration input were found to have a strong impact on its flood predictions (Section 3.5). This further demonstrates the importance of obtaining detailed soil data for urban flood modeling.

Stormwater infrastructure model input was also found to have a major influence on flood simulations. While the relative difference

Table 4
Average floodwater statistics for the scenario excluding stormwater infrastructure.

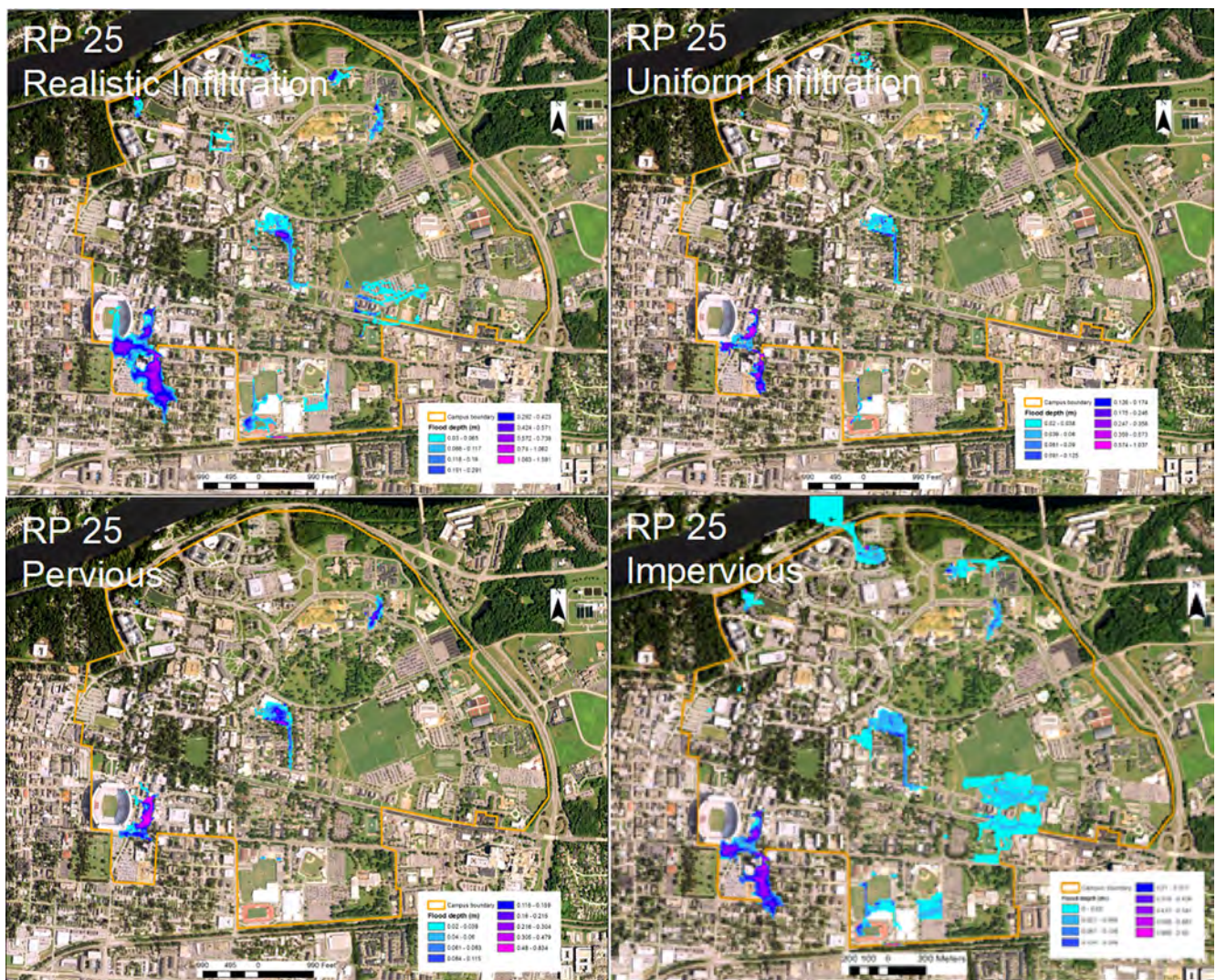| Flood scenario	No. of flooded cells	Average flood depth (m)	Maximum flood depth (m)	Floodwater volume (m^3)	Difference from realistic volume (Table 3) (m^3)	Volume difference ratio
RP 10	13,784	0.42	5.32	367,360	348,864	~20
RP 25	15,997	0.48	6.88	494,400	458,624	~14
RP 50	16,760	0.50	7.37	538,048	492,608	~12
RP 100	19,725	0.57	8.79	721,408	632,448	~8

Fig. 7. Maximum floodwater depth maps for the RP 25 scenario simulating different land-cover imperviousness settings.

between simulations which include and exclude stormwater infrastructure is reduced as storm magnitude increases, it remains of crucial importance even in high-magnitude events (a factor of 8 difference in floodwater volume predictions for RP100). The results highlight major challenges in urban flood predictions and analyses: obtaining detailed data on soil characteristics (mainly infiltration rate), obtaining detailed GIS data on stormwater infrastructure, and developing modeling frameworks that are able to simulate and couple both surface hydrology and subsurface drainage through the stormwater infrastructure. The latter is identified as a challenge given the costs and complexity of existing modeling frameworks. Emerging and future developments of national and global scale hyper-resolution flood forecasting and analysis frameworks, both in the US and internationally, mandate the development of solutions for obtaining high-resolution soil and

stormwater infrastructure data. These can include the development of data repositories and government mandates or incentives for local municipalities to update and share the data (somewhat akin to FEMA's National Flood Insurance Program), citizen science programs, and remote and proximity sensing analysis (e.g. Street View). Development of open-source alternatives to the commercial models will likely greatly improve accessibility to scientists and practitioners. Efforts should also focus on improving the computational efficiency and ease of use of the models through advances such as parallelization and cloud computing architecture and services.

5. Conclusion

Urban environments have highly heterogeneous infiltration rates

Table 5
Comparison of floodwater statistics for different land-cover settings.

Infiltration scenario	No. of flooded cells	Average flood depth (m)	Maximum flood depth (m)	Floodwater volume (m^3)	Ratio to realistic simulation volume
All impervious RP 25	3460	0.21	2.05	44,288	1.2
All pervious RP 25	774	0.13	0.83	6208	0.17
Uniform RP 25	975	0.11	1.04	6656	0.18
Uniform RP 100	3302	0.15	1.75	31,232	0.35
All impervious RP 100	6844	0.25	3.30	97,280	1.1
All pervious RP 100	3036	0.16	1.40	30,848	0.34

and complex drainage systems. Because of the general unavailability of detailed spatial data on infiltration and stormwater infrastructure, incorporating these characteristics into models of urban flooding is challenging. In this paper, we quantified the impact of stormwater infrastructure and soil infiltration on simulated flooding in an urban environment at a range of storm severities. We compared simulations in which stormwater infrastructure input was included and excluded; and soil infiltration inputs were configured differently (realistic, uniform, completely impervious and completely pervious). The results show that urban flood simulation is highly sensitive to inputs of both infiltration rates and stormwater infrastructure. Impact of stormwater infrastructure and infiltration values decrease for larger storms due to more rapid saturation of the stormwater infrastructure and soil. However, even for 100-year return period rainfall, the impact was very high; a factor of 8 greater simulated stormwater volume when excluding the stormwater infrastructure and about one-third of the simulated floodwater volume when using a spatially uniform infiltration input.

In light of these results we assert that there is a need to develop frameworks or mechanisms for making these urban datasets available and incorporating them into openly accessible and easy to implement hydraulic stormwater models. Such advances could greatly contribute to understanding of flood mechanisms in the urban environment and to prediction and management of flood risk in cities.

CRediT authorship contribution statement

Afrin Hossain Anni: Investigation, Software, Validation, Visualization, Writing - original draft. **Sagy Cohen:** Conceptualization, Writing - review & editing, Supervision, Resources, Funding acquisition, Project administration. **Sarah Praskievicz:** Conceptualization, Writing - review & editing, Supervision.

Declaration of Competing Interest

The authors declare that they have no known competing financial interests or personal relationships that could have appeared to influence the work reported in this paper.

Acknowledgments

References

ActionAid. Climate change, urban flooding and the rights of the urban poor in Africa, 2006.

Agbola, B.S., Ajayi, O., Taiwo, O.J., Wahab, B.W., 2012. The August 2011 flood in Ibadan, Nigeria: anthropogenic causes and consequences. International Journal of Disaster Risk Science 3, 207–217.

Al-Kaisi, M., Licht, M., 2005. Soil moisture conditions – consideration for soil compaction. Iowa State University IC-494 (9), 78–79.

Arnbjerg-Nielsen, K., 2012. Quantification of climate change effects on extreme precipitation used for high resolution hydrologic design. Urban Water Journal 9 (2), 57–65.

Arnone, E., Pumo, D., Francipane, A., La Loggia, G., Noto, L.V., 2018. The role of urban growth, climate change, and their interplay in altering runoff extremes. Hydrological Processes 32 (12), 1755–1770.

Bell, C.D., McMillan, S.K., Clinton, S.M., Jefferson, A.J., 2016. Hydrologic response to stormwater control measures in urban watersheds. Journal of Hydrology 541, 1488–1500.

Berggren, K., Packman, J., Ashley, R., Viklander, M., 2014. Climate changed rainfalls for urban drainage capacity assessment. Urban Water Journal 11 (7), 543–556.

Booth, R., 2012. Risk, planning for interdependencies: from theory to practice. Proceedings of the ICE-Municipal Engineer 165 (2), 85–92.

Brown, L., Murray, V., 2013. Examining the relationship between infectious diseases and flooding in Europe: a systematic literature review and summary of possible public health

interventions. Disaster Health 1 (2), 15–24.

Cadus, S., Poetsch, M., 2012. Dynamic modeling of urban rainfall runoff and drainage coupling DHI MIKE URBAN and MIKE FLOOD. University of Salzburg 1–52.

CEN, 1996. Drain and sewer systems outside buildings—Part 2: Performance Requirements, European Standard, European Committee for Standardization CEN, Brussels, Belgium.

CEN, 1997. Drain and sewer systems outside buildings—Part 4: Hydraulic design and environmental considerations, European Standard, European Committee for Standardization CEN, Brussels, Belgium.

Curriero, F.C., Patz, J.A., Rose, J.B., Lele, S., 2001. The association between extreme precipitation and waterborne disease outbreaks in the United States, 1948–1994. American Journal of Public Health 91 (8), 1194–1199.

Danish Hydraulic Institute (DHI). Business Management System, 2015. Storm Water Runoff from Green Urban Areas – Modelers Guideline. CRC for Water Sensitive Cities.

Danish Hydraulic Institute (DHI), 2017. Collection System. Modelling of storm water drainage networks and sewer collection systems. MIKE URBAN® user's guide, 2017.

Di Baldassarre, G., Montanari, A., Lins, H., Koutsoyiannis, D., Brandimarte, L., Blöschl, G., 2010. Flood fatalities in Africa: from diagnosis to mitigation. Geophysical Research Letters 37 (22).

EPA, 2018. https://www.epa.gov/water-research/storm-water-management-model-swmm.

EPA, 2019. Polluted Runoff: Nonpoint Source (NPS) Pollution- Low Impact Development, https://www.epa.gov/nps/urban-runoff-low-impact-development.

Fernández, D.S., Lutz, M.A., 2010. Urban flood hazard zoning in Tucumán Province, Argentina, using GIS and multicriteria decision analysis. Engineering Geology 111 (1–4), 90–98.

Fletcher, T.D., Shuster, W., Hunt, W.F., Ashley, R., Butler, D., Arthur, S., Trowsdale, S., Barraud, S., Semadeni-Davies, A., Bertrand-Krajewski, J.L., Mikkelsen, P.S., 2015. SUDS, LID, BMPs, WSUD and more–The evolution and application of terminology surrounding urban drainage. Urban Water Journal 12 (7), 525–542.

Galloway, E.G., Reilly, A., Ryoo, S., Riley, A., Haslam, M., Brody, S., Highfield, W., Gunn, J., Rainey, J., Parker, S., 2018. The Growing Threat of Urban Flooding: A National Challenge 2018. University of Maryland and Texas A&M University.

Grum, M., Jørgensen, A.T., Johansen, R.M., Linde, J.J., 2006. The effect of climate change on urban drainage: an evaluation based on regional climate model simulations. Water Science and Technology 54 (6–7), 9–15.

Hoang, L., Fenner, R.A., 2016. System interactions of stormwater management using sustainable urban drainage systems and green infrastructure. Urban Water Journal 13 (7), 739–758.

Huong, H.T.L., Pathirana, A., 2013. Urbanization and climate change impacts on future urban flooding in Can Tho city, Vietnam. Hydrology and Earth System Sciences 17 (1), 379–394.

IPCC, 2014. Impacts, adaptation, and vulnerability. Contribution of Working Group II to the Fifth Assessment Report of the Intergovernmental Panel on Climate Change, Cambridge University Press, Cambridge.

Li, C., Fletcher, T.D., Duncan, H.P., Burns, M.J., 2017. Can stormwater control measures restore altered urban flow regimes at the catchment scale? Journal of Hydrology 549, 631–653.

Liptan, T.W., 2017. Sustainable Stormwater Management: A Landscape-Driven Approach to Planning and Design. Timber Press.

Liu, W., Chen, W., Peng, C., 2014. Assessing the effectiveness of green infrastructures on urban flooding reduction: a community scale study. Ecological Modelling 291, 6–14.

LJWORLD, 2019. Organic matter content contributes to best topsoil, https:// www2.ljworld. com/news /2007/may/10/organic_matter_content_contributes_best_topsoil/.

Mahmood, M.I., Elagib, N.A., Horn, F., Saad, S.A., 2017. Lessons learned from Khartoum flash flood impacts: an integrated assessment. Science of the Total Environment 601, 1031–1045.

Mahmoud, S.H., Gan, T.Y., 2018. Urbanization and climate change implications in flood risk management: developing an efficient decision support system for flood susceptibility mapping. Science of The Total Environment 636, 152–167.

National Research Council, 2009. Urban Stormwater Management in the United States. National Academies Press.

NOAA, 2018. https://www.ncdc.noaa.gov/cdo-web/datatools.

Nouh, M., 2006. Wadi flow in the Arabian Gulf states. Hydrological Processes: An International Journal 20 (11), 2393–2413.

Ntelekos, A.A., Oppenheimer, M., Smith, J.A., Miller, A.J., 2010. Urbanization, climate change and flood policy in the United States. Climatic Change 103 (3–4), 597–616.

Schmitt, T.G., Thomas, M., Ettrich, N., 2004. Analysis and modeling of flooding in urban drainage systems. Journal of Hydrology 299 (3–4), 300–311.

Şen, Z., 2004. Hydrograph methods, arid regions, Saudi geological survey (SGS). Technical Report.

Teng, J., Jakeman, A.J., Vaze, J., Croke, B.F., Dutta, D., Kim, S., 2017. Flood inundation modelling: a review of methods, recent advances and uncertainty analysis. Environmental Modelling & Software 90, 201–216.

Tunstall, S., Tapsell, S., Green, C., Floyd, P., George, C., 2006. The health effects of flooding: social research results from England and Wales. Journal of Water Health 4, 365–380.

USDA, Soil survey field and laboratory methods manual, 2014. USDA, Soil survey investigation report no. 51, version 2; ASTM no. 1. 152H-type with Bouyoucos scale in g L-1 (developed by Stillwater, OK soil survey office and modified by NSSC and Ricky Lambert, Nacogdoches, TX).

Villarini, G., Smith, J.A., Baeck, M.L., Krajewski, W.F., 2011. Examining flood frequency distributions in the Midwest US 1. JAWRA Journal of the American Water Resources Association 47 (3), 447–463.

Walsh, C.J., Booth, D.B., Burns, M.J., Fletcher, T.D., Hale, R.L., Hoang, L.N., Livingston, G., Rippy, M.A., Roy, A.H., Scoggins, M., Wallace, A., 2016. Principles for urban stormwater management to protect stream ecosystems. Freshwater Science 35 (1), 398–411.

Weber, A., 2019. What is Urban Flooding? Natural Resources Defense Council (NRDC), https:// www.nrdc.org/experts/anna-weber/what-urban-flooding.

Yang, J.L., Zhang, G.L., 2011. Water infiltration in urban soils and its effects on the quantity and quality of runoff. Journal of Soils and Sediments 11 (5), 751–761.